Journal of Biomolecular NMR **27:** 175–179, 2003.

A combined HNCA/HNCO experiment for ^{15}N labeled proteins with ^{13}C at natural abundance

Eriks Kupce[a], D.R. Muhandiram[b] & Lewis E. Kay[b,*]
[a]*Varian Inc., Surrey KT12 2QF, U.K.;* [b]*Protein Engineering Network Centers of Excellence and Departments of Medical Genetics, Biochemistry and Chemistry, The University of Toronto, Toronto, Ontario, Canada, M5S 1A8*

Received 16 April 2003; Accepted 15 May 2003

Key words: cryogenic probe, HNCA, HNCO, ^{15}N and natural abundance ^{13}C protein samples, triple resonance NMR

Abstract

A triple resonance NMR experiment is presented for the simultaneous recording of HNCA and HNCO data sets on ^{15}N, natural abundance ^{13}C samples. The experiment exploits the fact that transfers of magnetization from ^{15}N to ^{13}CO and from ^{15}N to ^{13}C$^{\alpha}$ (and back) proceed independently for samples that are not enriched in ^{13}C. A factor of 2 in measuring time is gained by recording the two data sets simultaneously with no compromise in spectral quality. An application to a 0.5 mM ^{15}N labeled sample of protein-L is presented with all expected correlations observed in spectra recorded with a cryogenic probe at 500 MHz.

Communication

In comparison to other spectroscopic techniques NMR is inherently insensitive. However, in the past decade improved instrumentation and increasingly sophisticated multi-dimensional experiments have combined to greatly increase the scope of problems that can now be addressed using NMR methodology (Bax and Grzesiek, 1993; Wider and Wüthrich, 1999). The interplay between instrumentation and experiment is clearly apparent in the development of triple resonance spectroscopy (Kay et al., 1990). Implementation of ^{15}N, ^{13}C, ^{1}H experiments in the early 1990s required both new instrumentation and new experimental pulse schemes and labeling strategies. Typically, triple resonance experiments are performed on samples that are uniformly enriched to greater than 98% in both ^{15}N and ^{13}C (Bax and Grzesiek, 1993; Clore and Gronenborn, 1991). However, recent sensitivity gains resulting from higher magnetic fields, high sensitivity cryogenic probes, low noise-figure preamplifiers, and improved radio frequency performance, suggest that it may be possible to record some of the HNC-type triple resonance experiments on dilute ^{15}N, natural abundance ^{13}C samples in very reasonable measuring times. Indeed, as early as 1995 Led and co-workers presented a 2D H(N)CO experiment and recorded a ^{13}CO, ^{1}HN correlation spectrum of a 2 mM ^{15}N, natural abundance ^{13}C sample of the α3 Kunitz-type domain from human collagen (6 kDa), 30 °C, in 30 h (Kristensen et al., 1995). More recently, the feasibility of triple-resonance spectroscopy of uniformly ^{15}N, 10–20% ^{13}C labeled samples has been demonstrated using cryoprobe based technology (Anklin, 2002) and Prestegard and coworkers have developed a dipolar coupling based strategy for assignment and structure determination of ^{15}N, natural abundance ^{13}C protein samples (Tian et al., 2001). The approach was demonstrated on a 4.5 mM sample of rubredoxin (54 residues).

Herein, we describe a simultaneous HNCA/HNCO experiment that is optimized for ^{15}N labeled samples. Individual HNCA and HNCO correlation maps can be generated after acquisition by simple manipulations of the data set. The experiment is recorded on a *0.5 mM* sample of the B1 domain of peptostreptococcal protein L, a 62 residue polypeptide (Scalley et al., 1997) at 25 °C. All of the expected inter-residue

*To whom correspondence should be addressed. E-mail: kay@pound.med.utoronto.ca

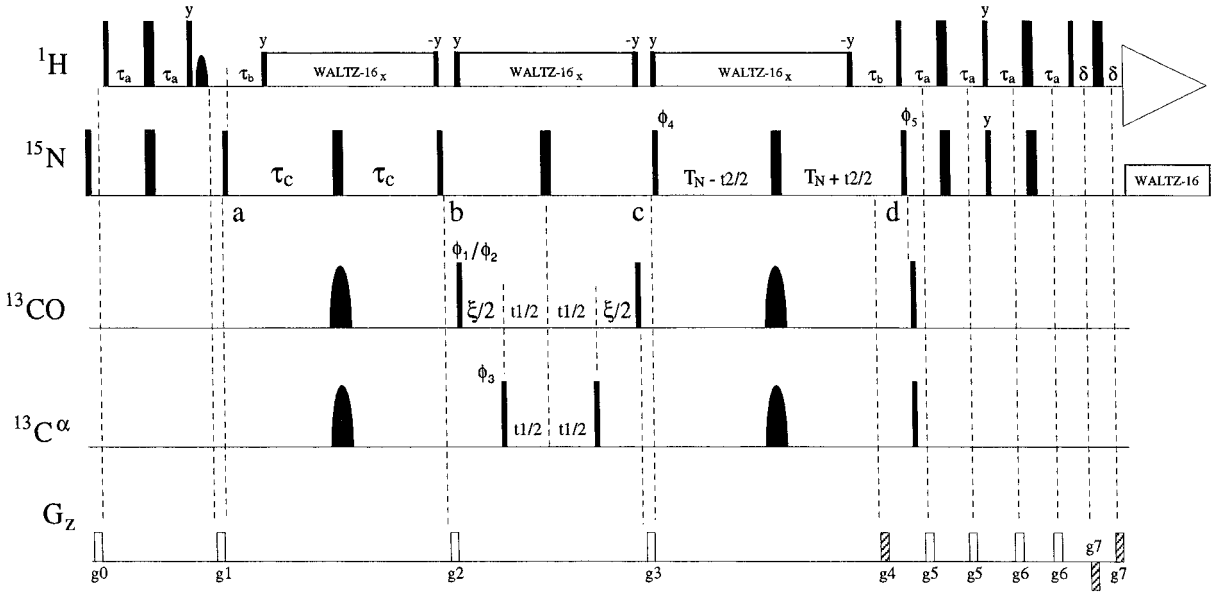

Figure 1. Pulse scheme used to record simultaneous HNCA/HNCO data sets. All narrow (wide) rectangular pulses are applied with flip angles of 90° (180°) along the x-axis unless indicated otherwise. The ^{1}H, ^{15}N and ^{13}C carriers are centered at 4.7 ppm (water), 119 ppm, and 58 ppm respectively. All proton pulses are applied with the highest field strength possible, with the exception of the WALTZ-16$_x$ decoupling element (Shaka et al., 1983) and the flanking pulses (applied with a 4.2 kHz field) and the water flip-back pulse prior to gradient g1 (1.7 ms 90° pulse). All ^{15}N pulses employ a 9 kHz field with decoupling achieved using an 840 Hz field. The ^{15}N 180° pulse between *c* and *d* is of the composite ($90_x180_y90_x$) variety. The shaped ^{13}CO and ^{13}C$^\alpha$ (180°) pulses were applied using a (single) 400 μs WURST pulse (Fu and Bodenhausen, 1995; Kupce and Freeman, 1995) with an 80 kHz sweep (11.2 kHz at maximum strength), centered at 117 ppm. All carbon 90° pulses employed a field of $\Delta/\sqrt{15}$ where Δ is the difference in Hz between the centers of the ^{13}CO and ^{13}C$^\alpha$ chemical shift regions (Kay et al., 1990), with the ^{13}CO pulses generated by rf phase modulation (Boyd and Soffe, 1989; Patt, 1992). The delays used are: $\tau_a = 2.4$ ms, $\tau_b = 5.5$ ms, $\tau_c = 15$ ms, $T_N = 15$ ms, $\delta = 500$ μs. The delay ξ is incremented as described in the text. The phase cycle employed is: $\phi1 = (x,-x)$, $\phi2 = (-x,x)$, $\phi3 = (x,-x)$, $\phi4 = x$, $\phi5 = x$, rec = (x,−x). Spectra are recorded in an interleaved manner using $\phi1$ and $\phi2$ as the phases of the first ^{13}CO 90° pulse and subsequently added and subtracted in the time domain to give HNCA and HNCO data sets, respectively. Quadrature in F_1 is achieved via States-TPPI (Marion et al., 1989) of $\phi1$,$\phi2$,$\phi3$, while quadrature in F_2 is achieved using the enhanced sensitivity gradient approach (Kay et al., 1992; Schleucher et al., 1993) with separate spectra recorded for ($\phi5$,g4) and ($\phi5$+180°,-g4). The phase $\phi4$ is incremented by 180° for each complex t_2 point. The gradient durations (ms) and strengths (G/cm) are: g0 = (0.5, 8), g1 = (0.5, 5), g2 = (0.75, 10), g3 = (1, 20), g4 = (1.25, 30), g5 = (0.3, 5), g6 = (0.4, 2.5) and g7 = (0.0625, 28.65).

(^{13}CO,^{15}N,^{1}HN; HNCO) and inter- and intra-residue (^{13}C$^\alpha$,^{15}N,^{1}HN; HNCA) correlations are observed in spectra acquired with a total measuring time of 22 h using a Varian spectrometer operating at 500 MHz equipped with a chiliprobe.

Figure 1 shows the enhanced-sensitivity pulsed field gradient-based experiment that has been developed for measuring HNCA/HNCO spectra. The pulse scheme is in many respects very similar to a large number of sequences that have been developed for application to uniformly ^{15}N, ^{13}C labeled proteins (Muhandiram and Kay, 1994; Schleucher et al., 1993) and in what follows we focus, therefore, on the differences between the present implementation and existing schemes. At point *a* in the sequence transverse ^{15}N magnetization is present which subsequently evolves due to couplings with ^{13}C$^\alpha$ and ^{13}CO spins. Since the sample is natural abundance in ^{13}C, evolution effectively results from only one of the following three couplings $\{^1J_{NC\alpha}, {}^2J_{NC\alpha}, {}^1J_{NCO}\}$. Thus, HNCO and HNCA pathways are independent and, further, in the case of the HNCA the intensities of the one- and two-bond correlations are not compromised by evolution resulting from $^2J_{NC\alpha}$ and $^1J_{NC\alpha}$, respectively. At point *b* the coherences that ultimately give rise to signal derive from terms of the form $2N_ZCO_Z$ (HNCO), $2N_ZC_Z^{\alpha(i)}$ (HNCA), $2N_ZC_Z^{\alpha(i-1)}$ (HNCA), where A_Z corresponds to longitudinal *A* magnetization and the superscripts (*i*) and (*i*−*1*) distinguish terms arising from $^1J_{NC\alpha}$ and $^2J_{NC\alpha}$, respectively. During the subsequent period extending between points *b* and *c* ^{13}CO and ^{13}C$^\alpha$ chemical shifts are recorded. By choosing

$$\begin{aligned} t_1(n) &= t_1(1) + (n-1)/\mathrm{sw}_{C\alpha}, \\ \xi(n) &= (n-1/2)[1/\mathrm{sw}_{CO} - 1/\mathrm{sw}_{C\alpha}] - 2\mathrm{pwc90}, \\ t_1(1) &= 0.5/\mathrm{sw}_{C\alpha} - (4/\pi)\mathrm{pwc90} - 2\mathrm{pwn90}, \end{aligned} \quad (1)$$

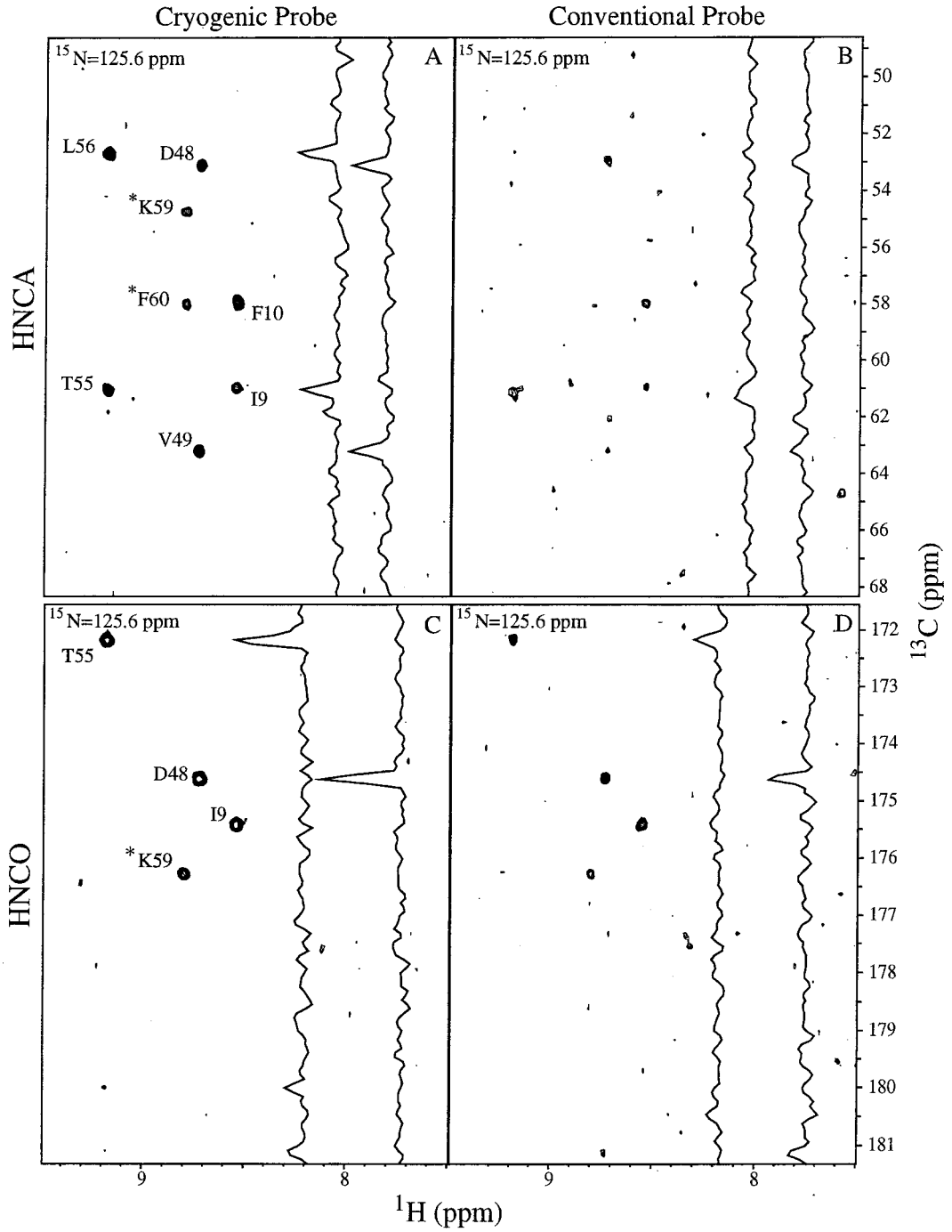

Figure 2. Comparison of data sets recorded using Varian chili- (A,C) and conventional, room temperature (B,D) triple resonance single axis gradient probe heads. Figures A,B (C,D) show HNCA (HNCO) planes at 125.6 ppm in the ^{15}N dimension recorded on a 0.5 mM ^{15}N, natural abundance ^{13}C sample of protein L at 25 °C, 500 MHz. Correlations are identified by the residue with the $^{13}C^{\alpha}$ or ^{13}CO chemical shift indicated on the vertical axis. Correlations denoted by * are more intense in an adjacent plane. A combined HNCA/HNCO data set was obtained with (64,32) complex points in each of t_1,t_2, 4 transients/FID and a relaxation delay of 1 s with spectra recorded in an interleaved manner using $\phi 1$ and $\phi 2$ as the phases of the first ^{13}CO 90° pulse. The total acquisition time for each of the chili- and conventional probe data set was 22 h (i.e., 22 h for the combined HNCA/HNCO). The interleaved data sets were separated using in-house written software and added/subtracted to generate HNCA/HNCO maps. Time domain spectra were processed using NMRPipe software (Delaglio et al., 1995) with standard processing macros. Of note, the spectra can be phased by applying 180° first order phase corrections in F_1 and by adjusting the zero order F_1 phase correction in the HNCO data set to reflect the fact that 90° $^{13}C^{\alpha}$ pulses are applied while ^{13}CO magnetization is in the transverse plane. The zero order F_1 phase correction in the HNCA is −90°.

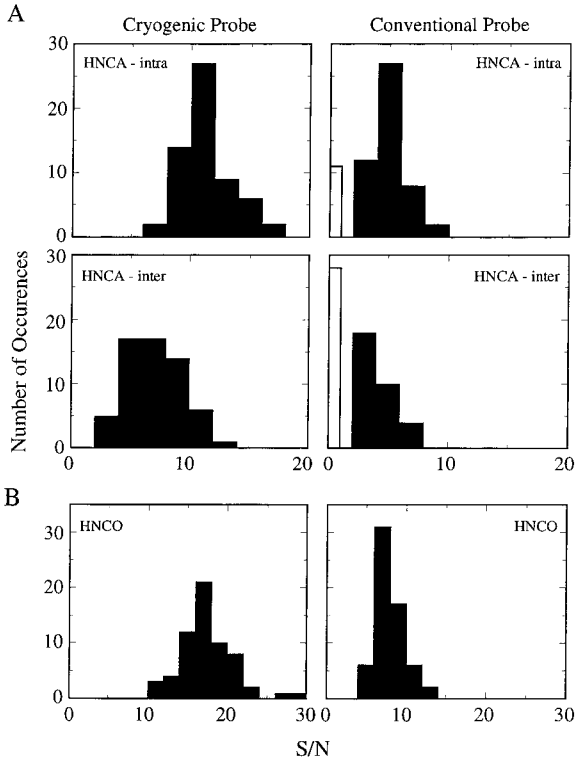

Figure 3. Histograms illustrating the signal-to-noise values of correlations in HNCA (A) and HNCO (B) spectra. All expected correlations are observed in spectra recorded with the cryogenic probe, while 82% and 55% of the HNCA-intra and HNCA-inter cross peaks, respectively, are above noise in data sets obtained with the regular (room-temperature) probe head. The white bars in A tabulate the number of residues for which correlations were not observed in data sets.

where $n = 1,2,\ldots$ denotes the point number, sw_{cj} is the spectral width in the cj dimension and pwc90, pwn90 are the ^{13}C and ^{15}N 90° pulse widths, it is possible to record spectra where the spectral widths in each of the two carbon dimensions (^{13}CO and $^{13}C^{\alpha}$) can be adjusted completely independently (so long as $\xi(n) \geq 0$). This is significant since our goal is to record spectra simultaneously without compromising quality. During this interval magnetization evolves as

$$A\cos(\omega_{CO}t_{1,CO}) + B\cos(\omega_{C\alpha(i)}t_{1,C\alpha}) + C\cos(\omega_{C\alpha(i-1)}t_{1,C\alpha}) \quad (2.1)$$

using the phase cycle $\phi1$, $\phi3$ (initial step) for the first ^{13}CO and $^{13}C^{\alpha}$ 90° pulses, respectively, and as

$$-A\cos(\omega_{CO}t_{1,CO}) + B\cos(\omega_{C\alpha(i)}t_{1,C\alpha}) + C\cos(\omega_{C\alpha(i-1)}t_{1,C\alpha}) \quad (2.2)$$

when the cycle $\phi2$, $\phi3$ is employed. In Equation 2, A, B and C are factors which include contributions from relaxation and the efficiency of magnetization transfer from ^{15}N to ^{13}C during the interval extending from *a* to *b*, and $t_{1,C\alpha}$, $t_{1,CO}$ emphasize the different spectral widths that are used for $^{13}C^{\alpha}$ and ^{13}CO. Note that the probability that a given ^{13}C spin is adjacent to a second is very low (~1%) so that the effects of ^{13}C-^{13}C couplings during t_1 can be ignored. This is one of the critical features that enables simultaneous acquisition of $^{13}C^{\alpha}$ and ^{13}CO chemical shifts with no degradation in spectral quality. Additionally, it is possible to employ significantly longer $^{13}C^{\alpha}$ evolution times than would be optimal in non-constant time HNCA applications recorded on uniformly ^{13}C labeled samples. Finally, magnetization is transferred back to ^{1}HN for detection, recording the ^{15}N chemical shift on route. In the present experiment separate data sets are recorded in an interleaved manner using the two phase cycles listed above. After addition and subtraction of the interleaved pair of data sets and subsequent processing an HNCA map is obtained with correlations of the form $\{\omega_{C\alpha(i)}, \omega_{N(i)}, \omega_{HN(i)}\}$, $\{\omega_{C\alpha(i-1)}, \omega_{N(i)}, \omega_{HN(i)}\}$ and an HNCO map with cross peaks at $\{\omega_{CO(i-1)}, \omega_{N(i)}, \omega_{HN(i)}\}$.

Figure 2 shows regions of 2D planes from HNCA and HNCO 3D spectra obtained on an ^{15}N, natural abundance ^{13}C, 0.5 mM sample of protein L, 50 mM

Na_3PO_4, pH 6.0, 0.05% NaN_3, 10% ^2H_2O, 25 °C. Spectra were recorded on Varian Inova 500 MHz spectrometers equipped with a cryogenic probe (*A*,*C*) or conventional room-temperature probe (*B*,*D*) using nearly identical parameters and the same total acquisition times (22 h). Figures 2A and B compare portions of HNCA planes (^{15}N chemical shift of 125.6 ppm). Only a few of the expected correlations are visible in the spectrum recorded using a regular probe head, while all of them are observed in the data set obtained with the cryogenic probe. The improved sensitivity is also evident in traces taken at ^{1}HN chemical shifts corresponding to L56 and V49, adjusted to the same noise level. Figures 2C,D show the corresponding HNCO planes. Notably, the intensities of correlations in the HNCO data set are higher than those in the HNCA since the $^{15}N \rightarrow {}^{13}C$ transfer times (between *a,b* and *c,d* in Figure 1) are optimized for the ^{15}N to ^{13}CO transfer. Indeed, all four of the expected HNCO correlations are observed in Figure 2D.

Figure 3 shows histograms of the distribution of signal-to-noise values of correlations obtained in the HNCA (A) and HNCO (B) data sets and on average the cryogenic probe data is a factor of 2.2 higher in sensitivity than the data recorded using a regular probe. While all of the expected correlations were observed in the cryogenic probe data sets, 82, 55 and 100% of the expected intra-HNCA, inter-HNCA and HNCO correlations were obtained in spectra recorded using the conventional room-temperature probe.

In summary, we have described a simple pulse scheme for recording HNCA and HNCO data sets simultaneously on reasonably dilute ^{15}N, natural abundance ^{13}C protein samples. A saving of a factor of two in time, relative to HNCA, HNCO data sets recorded individually, is realized using this approach. High quality data sets can be obtained, with ^{13}CO and $^{13}C^{\alpha}$ spectral widths optimized independently. It is expected that this experiment will be particularly valuable for applications involving structural studies of small proteins that do not express well in minimal media, thus precluding production of a ^{13}C-labeled sample, or in structural genomics initiatives where in addition to recording preliminary ^{1}HN-^{15}N HSQC spectra, HNCA/HNCO maps may be of interest as well.

Acknowledgements

This work was supported by a grant from the Canadian Institutes of Health Research. The authors thank Tony Mittermaier (University of Toronto) for sample preparation and AstraZeneca and Syngenta for generous financial support. L.E.K holds a Canada Research Chair in Biochemistry.

References

Anklin, C. (2002) *Experimental NMR Conference Poster 226. Triple Resonance NMR Experiments with Fractionally Carbon Labeled Proteins*. Asilomar, CA, April 2002.

Bax, A. and Grzesiek, S. (1993) *Acc. Chem. Res.*, **26**, 131.

Boyd, J. and Soffe, N. (1989) *J. Magn. Reson.*, **85**, 406–413.

Clore, G.M. and Gronenborn, A.M. (1991) *Science*, **252**, 1390–1399.

Delaglio, F., Grzesiek, S., Vuister, G.W., Zhu, G., Pfeifer, J. and Bax, A. (1995) *J. Biomol. NMR*, **6**, 277–293.

Fu, R., and Bodenhausen, G. (1995) *Chem. Phys. Lett.*, **245**, 415–420.

Kay, L.E., Ikura, M., Tschudin, R. and Bax, A. (1990) *J. Magn. Reson.*, **89**, 496–514.

Kay, L.E., Keifer, P. and Saarinen, T. (1992) *J. Am. Chem. Soc.*, **114**, 10663–10665.

Kristensen, S.O., Sorensen, M.D. and Led, J.J. (1995) *J. Biomol. NMR*, **5**, 411–414.

Kupce, E. and Freeman, R. (1995) *J. Magn. Reson.*, **A115**, 273–276.

Marion, D., Ikura, M., Tschudin, R. and Bax, A. (1989) *J. Magn. Reson.*, **85**, 393–399.

Muhandiram, D.R. and Kay, L.E. (1994) *J. Magn. Reson.*, **B103**, 203–216.

Patt, S.L. (1992) *J. Magn. Reson.*, **96**, 94–102.

Scalley, M.L., Yi, Q., Gu, H., McCormack, A., Yates, J.R. and Baker, D. (1997) *Biochemistry*, **36**, 3373–3382.

Schleucher, J., Sattler, M. and Griesinger, C. (1993) *Angew. Chem. Int. Ed. Engl.*, **32**, 1489–1491.

Shaka, A.J., Keeler, J., Frenkiel, T. and Freeman, R. (1983) *J. Magn. Reson.*, **52**, 335–338.

Tian, F., Valafar, H. and Prestegard, J.H. (2001) *J. Am. Chem. Soc.*, **123**, 11791–11796.

Wider, G. and Wüthrich, K. (1999) *Curr. Opin. Struct. Biol.*, **9**, 594–601.